Vapour reactive distillation process for hydrogen production by HI decomposition from HI–I2–H2O solutions

Bouchra Belaissaoui, Raphaële Théry Hétreux, Xuân-Mi Meyer, Michel Meyer, Vincent Gerbaud, Xavier Joulia

▶ **To cite this version:**

Bouchra Belaissaoui, Raphaële Théry Hétreux, Xuân-Mi Meyer, Michel Meyer, Vincent Gerbaud, et al.. Vapour reactive distillation process for hydrogen production by HI decomposition from HI–I2–H2O solutions. Chemical Engineering and Processing: Process Intensification, 2008, 47 (3), pp.396-407. 10.1016/j.cep.2007.01.018 . hal-02943401

HAL Id: hal-02943401
https://hal.science/hal-02943401

Submitted on 20 Mar 2024

HAL is a multi-disciplinary open access archive for the deposit and dissemination of scientific research documents, whether they are published or not. The documents may come from teaching and research institutions in France or abroad, or from public or private research centers.

L'archive ouverte pluridisciplinaire **HAL**, est destinée au dépôt et à la diffusion de documents scientifiques de niveau recherche, publiés ou non, émanant des établissements d'enseignement et de recherche français ou étrangers, des laboratoires publics ou privés.

VAPOUR REACTIVE DISTILLATION PROCESS FOR HYDROGEN PRODUCTION BY HI DECOMPOSITION FROM HI-I_2-H_2O SOLUTIONS

B. BELAISSAOUI, R.THERY, X.M. MEYER[1], M. MEYER, V. GERBAUD and X. JOULIA

LGC-Laboratoire de Génie Chimique, UMR CNRS 5503

5 rue Paulin Talabot 31106 Toulouse Cedex 1, France

Phone : + 33 5 62885826; Fax : + 33 5 62885600

E-mail: XuanMi.Meyer@ensiacet.fr

Accepted for publication in Chem. Eng. Proc., 47(3), 396-407, 2008

ABSTRACT

In this contribution, a sequential and hierarchical approach for the feasibility analysis and the preliminary design of reactive distillation columns is extended to systems involving vapour phase chemical reaction and is successfully applied to the HI vapour phase decomposition to produce H_2.

The complex phase and physico chemical behaviour of the quaternary HI-H_2-I_2-H_2O system is represented by the Neumann's thermodynamic model and instantaneous vapour phase chemical equilibrium is assumed.

Then, from minimal information concerning the physicochemical properties of the system, three successive steps lead to the design of the unit and the specification of its operating conditions: the feasibility analysis, the synthesis and the design step. First, the analysis of reactive condensation curve map method (rCCM*),* assuming infinite internal liquid and vapour flow rate and infinite reflux ratio, is used to assess the feasibility of the process. It determines the column structure and estimates the attainable compositions. These results are used as inputs data for the synthesis step. Based on the boundary value

design method (BVD), considering finite internal liquid and vapour flow rate and finite reflux ratio while neglecting all thermal effects and assuming a constant heat of vaporisation, the synthesis step provides more precise information about the process configuration (minimum reflux ratio, number of theoretical stages, localisation and number of reactive plates, position of the feed plate). Finally, the BVD method results are used to initialise rigorous simulations, based on an equilibrium stage model with energy balance, to estimate the reflux ratio taking into account thermal effect on the process.

The resulting design configuration consists in a single feed and entirely reactive distillation column. The column operates under a pressure of 22 bars. The feed of the reactive distillation column, coming from the Bunsen reaction section [x_{HI}=0.10; x_{I2}=0.39 x_{H2O}=0.51], is at its boiling temperature. The residue consists in pure iodine. Water and produced hydrogen are recovered at the distillate. The column operates at a reflux ratio of 5 and is composed of 11 theoretical plates including the reboiler and the partial condenser with the feed at the stage 10 (counted downwards). The obtained HI dissociation yield is 99.6%.

Keywords: Hydrogen production, Sulfur/Iodine thermochemical cycle, vapour phase reactive distillation, reactive distillation design.

1. INTRODUCTION

In the current context of increasing energy demand, new solutions leading to reduce greenhouse effect gas emission are investigated. Among various alternatives, hydrogen appears as one of the most attractive energy vector for the future. The thermochemical water decomposition cycle using nuclear heat is one of the processes for hydrogen production from water. Hydrogen can be obtained from water at temperatures lower than the direct water decomposition (~4000K) by combining a set of coupled thermally-driven chemical reactions.

The sulfur/iodine (S/I) thermochemical cycle is a promising one [1] . The cycle inputs are heat and water. The outputs are hydrogen and oxygen. It consists of three main reactions with the recycling of iodine and sulphur dioxide as shown in figure 1 :

$$9\ I_2 + SO_2 + 16\ H_2O \rightarrow (2\ HI + 10\ H_2O + 8\ I_2) + (H_2SO_4 + 4\ H_2O) \qquad [393K] \qquad (R_1)$$

$$2\ H_2SO_4 \rightarrow 2\ SO_2 + 2\ H_2O + O_2 \qquad [1123K] \qquad (R_2)$$

$$2\ HI \leftrightarrow H_2 + I_2 \qquad [723K] \qquad (R_3)$$

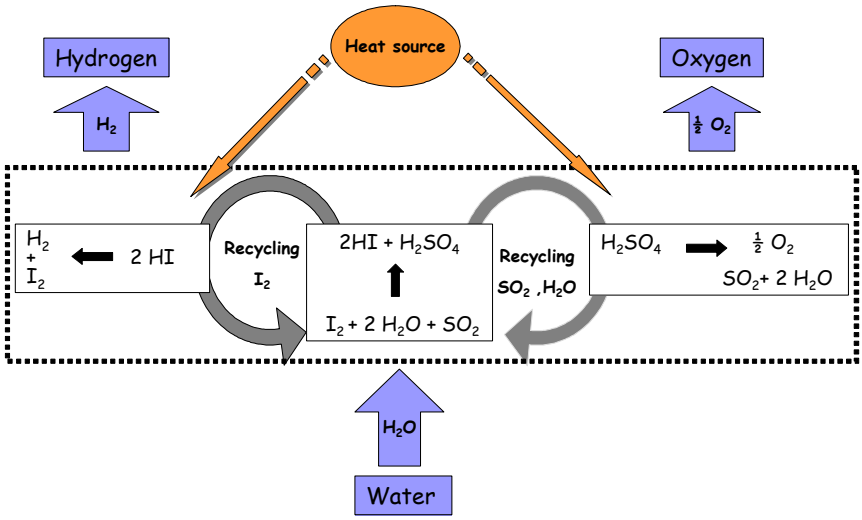

Figure 1. The principle of the thermochemical water decomposition cycle for hydrogen production

The hydrogen production process design leads to three sections as illustrated on figure 2.

In section I, the first reaction R_1, called the Bunsen-reaction, proceeds exothermically in a liquid phase and produces two immiscible acid phases: the hydroiodic acid and sulphuric acid phases. After separation, these acid phases are concentrated and decomposed in sections II and III according to reactions R_2 and R_3. In section II, Reaction R_2 is the endothermic H_2SO_4 decomposition into water, oxygen and sulphur dioxide and takes place in a gas phase catalytic reactor. In section III, the HI phase is first concentrated by distillation and the HI-H_2O distillate at azeotropic composition (13% molar in HI) is decomposed in the vapour phase according to reaction R_3 which we focus on in this work. It is a catalytic and equilibrium limited reaction with a small endothermic heat of reaction. Except for hydrogen and oxygen, the products of the R_2 and R_3 and the excess of water and iodine are recycled as reactants in the Bunsen-reaction step.

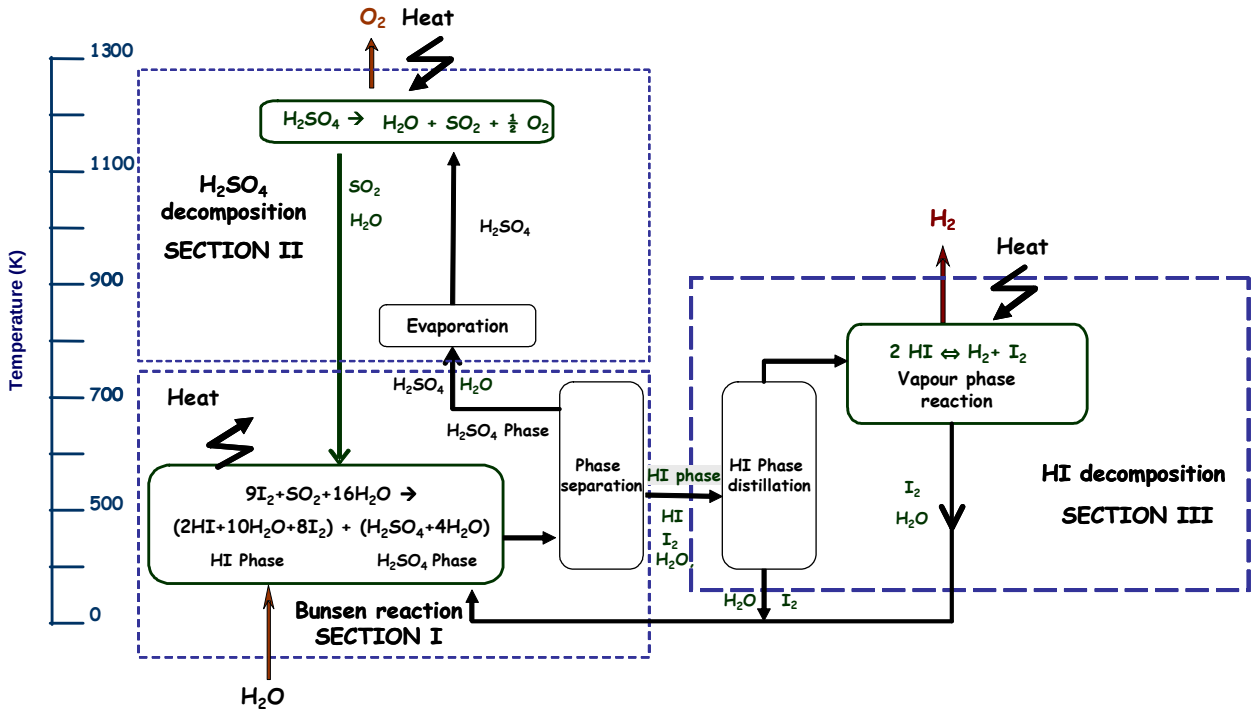

Figure 2. Concept of the Sulfur / Iodine thermochemical cycle for the production of hydrogen

The HI concentration and decomposition section (section III) is one of the most expensive and energy consuming steps of this cycle and suffers several drawbacks:

(1) The HI decomposition degree is limited by the chemical equilibrium and the conversion at 723K does not exceed 22.4%

(2) An excess of iodine and water is needed for the separation of the two phases after the Bunsen reaction R_1. Therefore, a large amount of H_2O and iodine is recycled to the Bunsen reaction from the HI distillation column. At least, an excess of 8 moles of I_2 and 14 moles of H_2O are necessary to produce one mole of hydrogen.

(3) The HI purity of the azeotropic distillate input to reaction R_3 obtained is low (13% molar). A lot of energy is required to evaporate the water in excess.

Several alternatives have been proposed in order to improve the efficiency of the process in section III.

In order to improve the concentration of the HI phase after the Bunsen reaction, the General Atomic Co group proposed the use of phosphoric acid (H_3PO_4) for the concentration of the HI solution [2]. A

vapour with a 99.7% molar in HI was obtained. But, the remaining H_3PO_4 solution was concentrated by using large amounts of heat and electricity. An electro-electrodialysis (EED) concentration method was also proposed by Arifal et al. (2002) [3] and Onuki et al. (2001) [4]. Improvement of the HI decomposition reaction conversion was also investigated using a H_2 permselective membrane reactor by Hwang and Onuki (2001) [5].

Another proposal aimed at reducing the stream obtained at the top of the HI distillation column by concentrating HI over the azeotropic I_2-H_2O composition before reaction R_3. Indirectly achieving this goal, reactive distillation was first proposed and investigated by Roth and Knoche (1989) [6]. It consists to replace both distillation and decomposition steps in the S/I cycle (see figure 3). In this integrated process, HI is directly decomposed in the vapour phase from the HI-I_2-H_2O solution [x_{HI}=0.10; x_{I2}=0.39 x_{H2O}=0.51] coming from the Bunsen reaction in section I.

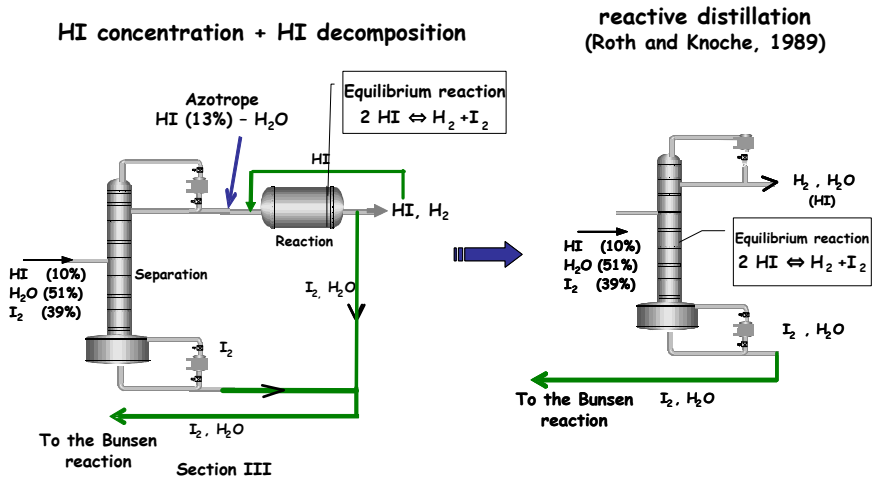

Figure 3: Integration of a reactive distillation in the Sulfur / Iodine thermochemical cycle for the production of hydrogen

Combining reaction and separation in a single apparatus of reactive distillation presents numerous advantages: the continuous removal of one of the products from the reacting mixture shifts the equilibrium towards the production of I_2 and H_2 and enables to increase the conversion of HI and reduce the recycling of vapour HI.

The purpose of this article is to apply the design approach devised by Thery *et al.*(2005) [7] extended to vapour phase reaction to the HI vapour phase decomposition to produce H_2.

First, the general consideration of the thermodynamic of the HI-H_2-I_2-H_2O system is presented. A synthesis of the available experimental data for this system in the literature is reported. The adopted model in the present work is exposed. A comparison between model calculation and experimental data is also presented. Second, the extended design approach is used to propose a preliminary design for the reactive distillation column. Results for each step of the design procedure are commented. Finally, the conclusion and perspectives of the present work are emphasized.

2. THERMODYNAMICS OF HI-H_2-I_2-H_2O SYSTEM

2.1. Thermodynamic and chemical behaviour of HI-H_2-I_2-H_2O system

The HI-H_2-I_2-H_2O system thermodynamic behaviour is complex as a vapour-liquid-liquid-solid phase coexistence system occurs in the catalytic reactive distillation column. The solid phase is not considered in this work and figure 4 hints at the remaining complexity. Besides thermodynamic phase behaviour is characterised namely by:

- Highly immiscible H_2O-I_2 liquid-liquid equilibrium
- Azeotropic H_2O-HI binary exhibiting liquid-liquid equilibrium
- High temperature triple point for I_2 (387K)
- HI-I_2-H_2O ternary mixture displays two separate liquid-liquid regions.

In the HI-H_2-I_2-H_2O system, several chemical reactions occurs and class it among the strong electrolytic systems:

- Vapour phase HI equilibrium decomposition: $2HI \leftrightarrow I_2+H_2$.
- Polyiodide ions formation: $I_2 + I^- \leftrightarrow I_3^-$, $I_2 + H^+ \leftrightarrow I_2H^+$.
- Ion solvation: $5\ H_2O + HI \leftrightarrow (5\ H_2O, H^+) + I^-$

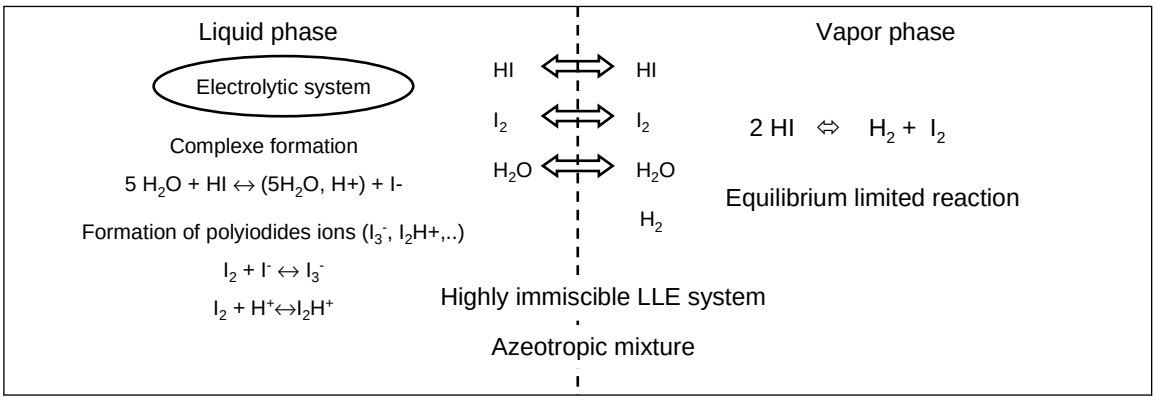

Figure 4. Description of the complex phase behaviour of the HI-H_2-I_2-H_2O system

2.2. Available experimental data for the HI-I_2-H_2O ternary system

The I_2-H_2O system has been studied by Kracek [8] in 1931. The solubility of iodine in water was measured and a miscibility gap lying between the solid-liquid equilibrium point at 385.4K (close to the melting point of iodine: 386.8K) and an upper temperature of approximately 553K was detected. At 385.4K, the light aqueous phase contains 0.05% molar of iodine and the heavy phase about 98% molar of iodine.

Total pressures of HI-H_2O mixtures have been investigated by Wüster and Vanderzee [9-10]. This system exhibits an azeotrope whose precise composition depends on temperature and pressure. A synthesis of these data has been published by Engels and Knoche (1986) [11]. In the ternary HI-I_2-H_2O system recently reviewed by Mathias (2005) [12] (see figure 4), the liquid phase exhibits two immiscibility regions which are the extension of the partly miscible systems I_2-H_2O and HI-H_2O: one for low HI contents, due to the very low miscibility of I_2 in H_2O, and the second one, for high HI contents and about H_2O/I_2 of 30% concentration. The first one tends to disappear with increasing HI concentration probably because of the formation of polyiodides ions like I_3^- or I_2H^+. No data are available for the liquid-liquid equilibrium in the miscibility region with low HI content.

Engels and Knoche (1986) [11] have performed total pressure measurements for the HI-H_2O-I_2 ternary system for various iodine concentrations in the $0 \leq x_{HI}/x_{H2O} \leq 0.19$ molar compositions and $393K \leq T \leq 573K$ temperature domain.

They have found that the dissociation of gaseous HI shifts the HI composition towards lower HI contents than is expected from the binary HI-H_2O azeotrope. Starting from the binary HI-H_2O, they have shown

that the line of vapour pressure minima of the system goes through the entire concentration field towards the pure iodine. They called the HI compositions on this line the pseudo-azeotropic compositions.

Engels and Knoche (1986) [11] have found that for HI concentrations higher than the pseudo-azeotropic composition, the vapour phase is very rich in HI, and for high temperatures (>473K), HI might be dissociated in the vapour phase in H_2 and I_2.

They have also found that comparing to the homogeneous gas phase reaction, higher hydrogen partial pressures are reached in the case of the direct decomposition from HI-H_2O-I_2 solutions with HI content greater than the pseudo-azeotropic composition and for low iodine content. They explained this observation by the fact that the liquid absorbs most of iodine from the vapour and so the reaction equilibrium of the HI decomposition is shifted strongly to the right side. This result is in agreement with further experiments done by Berdhauser and Knoche [13].

The HI decomposition is slightly endothermic, thus the chemical equilibrium is promoted by high temperatures. The kinetic of this reaction is very slow and the use of appropriate catalyst permits to approach rapidly the chemical equilibrium conversion.

The HI decomposition reaction has been extensively investigated from the early 1900s to the present day. Extensive experimental work on the heterogenous decomposition of HI including catalyst research program, applied specifically to thermochemical water splitting, has been extensively conducted at two laboratories : the National Chemical Laboratory for Industry, Japan, and General Atomics, United States. Results are reported by O'Keefe *et al.* (1980)[14].

2.3. The adopted thermodynamic model: Neumann's model (1987)

In this study, we consider the thermodynamic model proposed by Neumann (1987) [15]. It is based on the following assumptions:

- the vapour phase is ideal, despite high total pressures
- in the liquid phase, a solvation equilibrium occurs: $5\ H_2O + HI \leftrightarrow (5H_2O, H^+) + I^-$
- the polyiodide formation is neglected : $I_2 + I^- \leftrightarrow I_3^-$, $I_2 + H^+ \leftrightarrow I_2H^+$

The non ideality of the liquid phase is represented by the NRTL activity coefficient model with binary interaction parameters (including solvent-complex) estimated from the experimental vapour - liquid data computed by Engels and Knoche (1986) [11].

Neumann [15] has identified two sets of parameters corresponding respectively to two temperature ranges: below and above 423K. He has also identified the expression of the solvation equilibrium constant $K_a(T)$,

$$\ln K_a(T) = -8.549 + 6692/T \qquad [1]$$

with T in K.

The HI decomposition reaction is an equilibrium limited reaction taking place in the vapour phase. The chemical equilibrium constant is expressed as the ratio of the partial pressure P_i of the component i:

$$K_{eq} = \frac{P_{H_2}.P_{I_2}}{P^2_{HI}} \qquad [2]$$

The expression of the HI decomposition chemical equilibrium constant as a function of the temperature T has been proposed by Neumann (1987) [15] and is expressed as follows:

$$\ln K_{eq}(T) = -0.03684 - 2772.7729/T \qquad [3]$$

with T in K.

However, modelling inadequacies as well as a lack of fundamental data [12] lead to a non predictive and non validated behaviour of the vapour – liquid – liquid equilibria that are known to occur. A more reliable and accurate thermodynamic model for the studied system remains a challenge and the current model of Neumann can only be safely applied to perform vapour – liquid calculations.

2.4. Comparison between model calculation and experimental data

In figure 5, we compare the experimental data of Engels et Knoche (1986) [11] with Neumann's model calculation. In this figure, the non reactive diagram P-x-y of the binary HI-H_2O for the temperatures of 450K , 500K and 550K is reported. The points are the experimental data where the dissociation of HI is negligible. The model is clearly able to capture the azeotropic behavior of the system. Thus the model is

able to describe the liquid-vapour equilibrium for systems with $0 \leq x_{HI}/x_{H2O} \leq 0.19$ and temperatures range to 393K and 573K at various iodine concentrations corresponding to the experiments available domain.

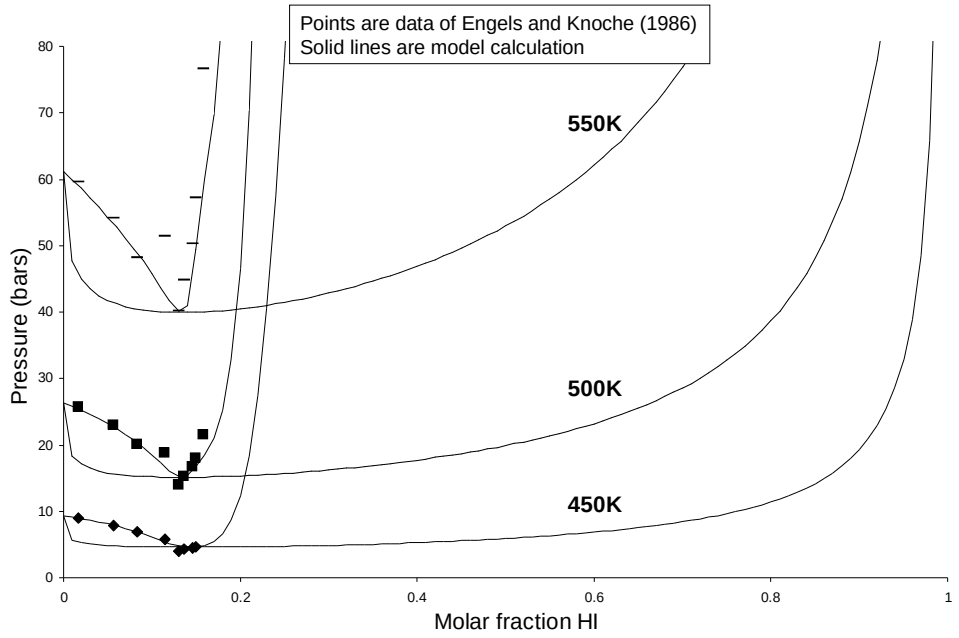

Figure 5. Diagram P-x-y of HI-H_2O. Comparison of the Neumann's thermodynamic model calculation to experimental data of Engels and Knoche (1986)

3. THE EXTENDED APPROACH FOR THE DESIGN OF VAPOUR PHASE REACTIVE DISTILLATION COLUMN

During the past decades, many methods have been proposed for the feasibility analysis and the design of RD processes [16-17]. Thery et al. [7] have developed a sequential and hierarchical approach for the design of reactive distillation column involving liquid phase reactions. In the context of this study, the different steps constituting the design approach have been extended to systems involving vapour phase chemical reactions [18]. Figure 6 presents a flow chart of the approach.

A key interest of this methodology lies on a progressive introduction of the process complexity. From minimal information concerning the physicochemical properties of the system, three steps lead to the design of the unit and the specification of its operating conditions : the feasibility analysis, the synthesis step and the design step.

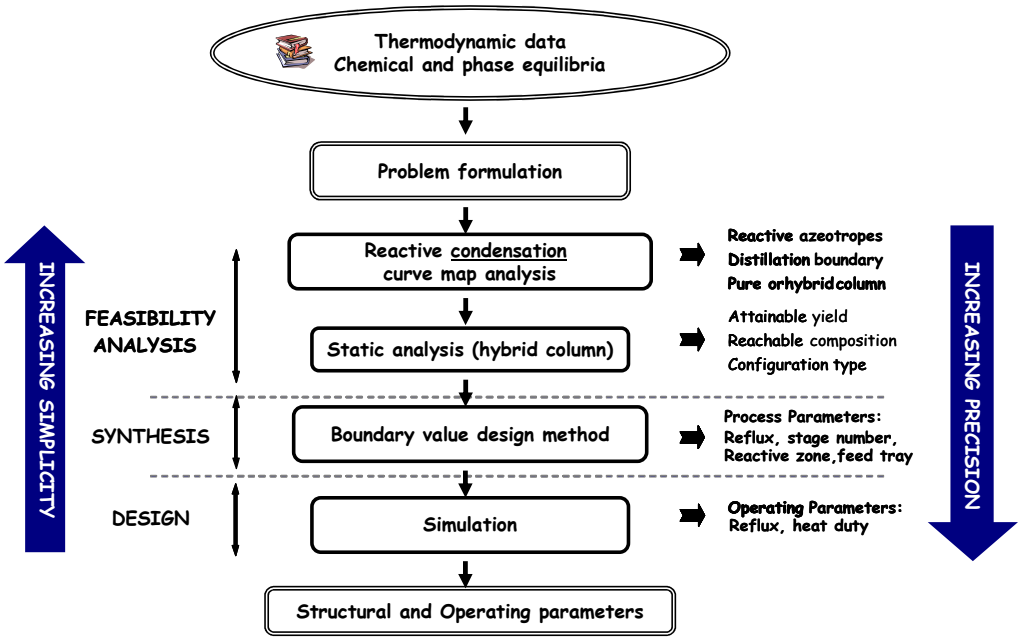

Figure 6. Methodology for the design of vapour phase reactive distillation processes.

3.1. Feasibility Analysis

3.1.1. Analysis of the reactive condensation curve map

The qualitative analysis of the reactive residue curve map (rRCM) first proposed by Barbosa and Doherty [19] can be readily used. However, because the reaction occurs in the vapour phase, condensation curve separatrices should be analysed instead of residue curve separatrices [20]. The reactive condensation curve map (rCCM) are computed by simulating an open condensation process experiencing equilibrium reaction for various initial vapour compositions and by representing the locus of vapour composition in physical and chemical equilibrium with the liquid phase. The feasibility analysis aims at making sure that the specifications are physically attainable. It defines the most favourable feed composition and the column structure necessary to obtain the desired product (requirement of a pure separation section, requirement of one or two feed plates).

3.1.2. Static Analysis

The static analysis (SA) method assesses the feasibility of partially reactive columns. Assuming infinite flowrates, the composition profile in the column can be represented by the distillation line. The obtained number of stages corresponds to the minimal number of stages. The method enables to determine the attainable extent of the reaction, the distillate and bottom products compositions and hints at the column

configuration (approximate number of stages, localization and size of the reactive zone). The SA method assumptions [21] hold whatever the reactive phase, so that its extension to handle vapour phase reaction is straight forward, the mixture resulting from the reaction step and entering the separation device being then in vapour state.

3.2. Synthesis step

The synthesis step is based on the boundary value design (BVD) method that provide precise information about the process configuration and characteristics (minimum and maximum reflux ratios, number of theoretical stages, localisation and number of reactive plates, position of the feed plate). Constant Molar Overflow (CMO) assumptions are formulated so that thermal effects are not considered and composition profiles are deduced from the mass balance equations [22-23].

Furthermore, assuming instantaneous vapour phase equilibrium, transformed composition variables [24] can be used.

3.3. Design Step

Thermal phenomena (heat of reaction, difference between components vaporisation enthalpy…) have been ignored so far and are considered in the design step, through the introduction of energy balances in a MESH model suitable for simulation. The former steps have set the column configuration and the design step aims at adjusting the operating parameters taking into account the overall complexity of the process. Simulation is carried out using ProSimPlus® [25]. Given the pressure and the column configuration, the degree of freedom of the MESH model is equal to 2: to saturate this degree of freedom, the purity and the partial flow rate of the desired component (at the top or at the bottom) are fixed. Then, the required reflux ratio and heat duties are deduced from the model resolution. To help the calculations, compositions and temperature profiles estimated during the synthesis step are used as initialization points. At the end of this step, a column structure and the associated operating parameters necessary to achieve the initial specifications are available.

4. APPLICATION OF THE DESIGN APPROACH TO THE HYDROIODIC ACID-HYDROGEN-IODINE–WATER SYSTEM

In this section, we present the results of the application of the extended reactive distillation design approach to the hydroiodic acid - hydrogen – iodine – water system.

4.1. Pressure Choice

Because remarkable hydrogen partial pressures are only found for solutions with a HI content higher than the azeotropic molar fraction [11], an operating pressure of 22 bars has been proposed by Roth and Knoche [6]. It corresponds to the minimum pressure of the boiling feed stream (with composition fixed by the Bunsen reaction [x_{HI}=0.10; x_{I2}=0.39 x_{H2O}=0.51]) in order to have a HI molar fraction suitable for the production of hydrogen. The global design approach is applied below for this pressure.

4.2. Feasibility analysis

4.2.1. Non reactive condensation curve map (nrCCM) of the ternary HI-I_2-H_2O system

The non-reactive condensation curve map of the HI-I_2-H_2O system under the pressure of 22 bars is represented on the figure 7. It exhibits four singular points, namely the three pure components, iodine, water and hydroiodic acid and the binary azeotrope HI-H_2O ($T_{boiling}$=518.28K; x_{HI}=0.133 molar).

This binary azeotrope stability is a saddle which generates a non reactive boundary distillation and leads to two distillation regions. In the first distillation region, H_2O is a stable node. In the second distillation region, HI is a stable node. I_2 is a unstable node in both distillation region.

Figure 8 shows the influence of the I_2 concentration on the maximum bubble temperature of the ternary system HI-I_2-H_2O. The crest, corresponding to the non reactive boundary distillation of the HI-I_2-H_2O system, relies the pure iodine point (T=642.32K) to the binary azeotrope HI-H_2O (T=518.28K). This result is in agreement with the one obtained from the non reactive Condensation Curve Map (nrCCM) of the ternary HI-I_2-H_2O system.

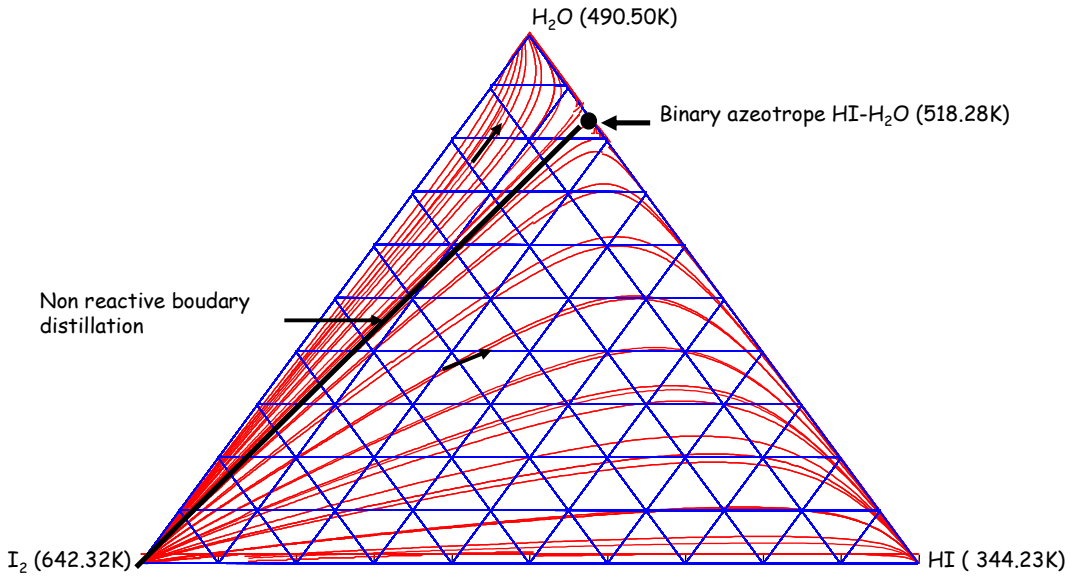

Figure 7. Non reactive condensation curve map of the ternary HI-I_2-H_2O system under 22 bars

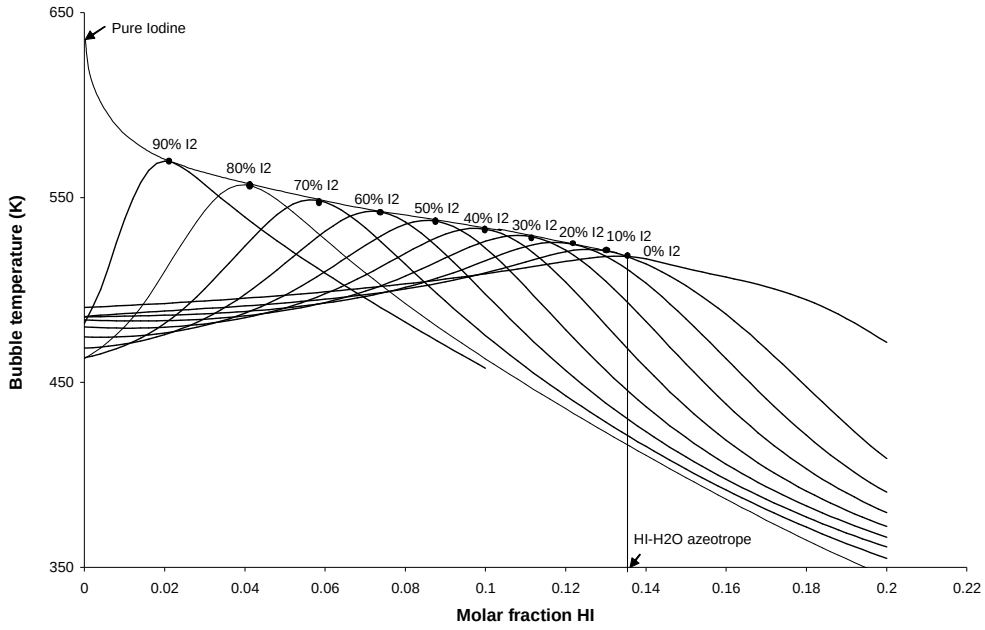

Figure 8. Influence of I_2 concentration on the maximum bubble temperature of the non reactive ternary system HI-I_2-H_2O

4.2.2 Reactive condensation curve map (rCCM) of the quaternary HI-H_2-I_2-H_2O system.

4.2.2.1. Singular points

The reactive condensation curve map of the hydroiodic acid-hydrogen-iodine-water system under the pressure of 22 bars is presented on figure 9. This *r*CCM is represented using reactive compositions [24]

noted $\overline{X}$ and $\overline{Y}$ for the liquid and the vapour phase respectively. Each point inside the diagram characterizes an equilibrium mixture. The binary edges I_2-H_2O and H_2-H_2O refer to non reactive mixtures whereas the binary edge I_2-H_2 refers to the HI decomposition reaction. Iodine, hydrogen and water appear as vertices (respectively, unstable, stable and saddle singular points) but no vertex corresponds to pure HI because HI can not exist alone in the mixture under the chemical equilibrium. Finally, the binary azeotrope HI-H_2O can not exist anymore in the *r*CCM because of the HI decomposition.

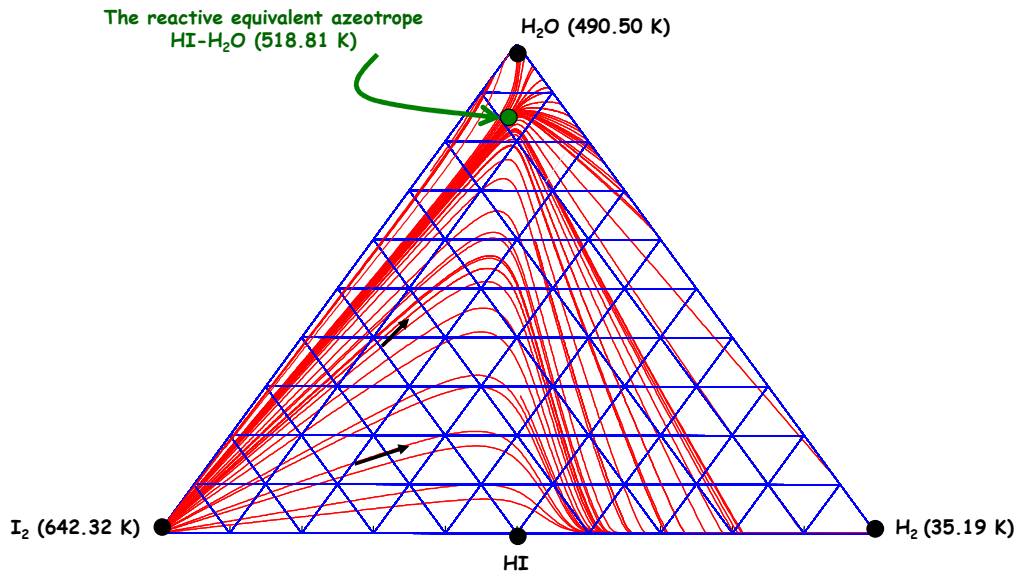

Figure 9. Reactive condensation curve map (rCCM) of the HI-H_2-I_2-H_2O system under 22 bars.

A closer look at figure 9 shows that another attraction point exists inside the reactive composition space.

The condensation curves are heavily curved near this point but they do not stop on it and move toward the stable node hydrogen. As illustrated on figure 10, the $X_{I_2} - Y_{I_2}$ curve nears this point without intersecting the X=Y straight line. It can though be qualified as a saddle point.

This singular point is the "equivalent reactive azeotrope" of the binary azeotrope HI-H_2O, it results from the decomposition of HI in the binary azeotrope HI-H_2O into H_2 and I_2 as illustrated in table 1 comparing the vapor physical composition of equivalent reactive azeotrope with those of the binary azeotrope. Indeed, the HI molar composition of the equivalent reactive azeotrope is lower than in the binary azeotrope and the difference corresponds to the some of I_2 and H_2 molar fraction in the equivalent

reactive azeotrope. According to the steoechiometry of the reaction, the I_2 and H_2 molar fraction are equal. Because H_2O is an inert in this case, its molar fraction remains the same. The equivalent reactive azeotrope is at the temperature of 518.81K while the binary azeotrope HI-H_2O is at 518.28K.

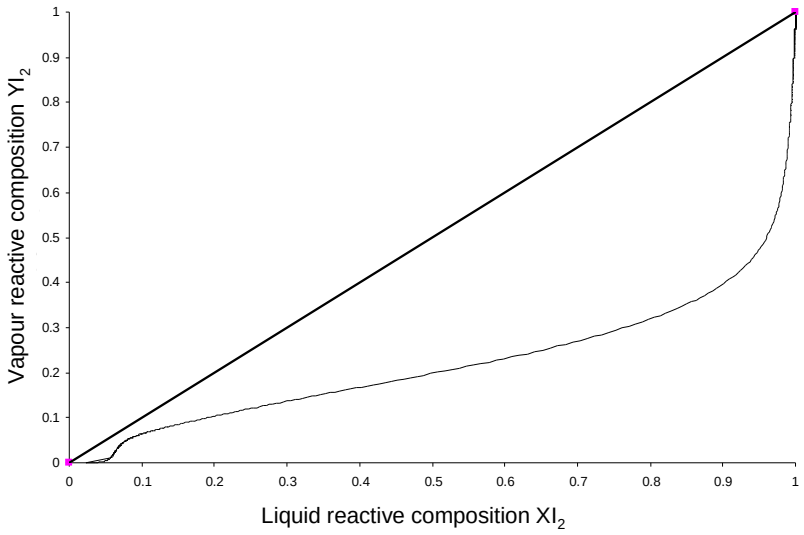

Figure 10. X_{I_2} - Y_{I_2} diagram of the HI-H_2-I_2-H_2O system under 22 bars

Table 1. Approximated vapor physical composition of the equivalent reactive azeotrope compared to the binary azeotrope (P=22bars)

	HI	H_2	I_2	H_2O
Equivalent reactive azeotrope	0.1170	0.0080	0.0080	0.8670
Binary azeotrope	0.1330	0.0000	0.0000	0.8670

4.2.2.2. Feasible specifications

The vapour-liquid region where the thermodynamic model is considered reliable is shown on figure 11, it is the miscibility zone inside the delineated liquid reactive composition region.

According to the feasibility rules introduced by Ung and Doherty [26], a reactive distillation process is feasible at total reflux if in the reactive composition space, the distillate (D), feed (F) and bottom (B) points are aligned and if D and B belong to the same reactive condensation curve.

As the feed composition is given by the Bunsen reaction step (point F in figure 11), reachable specifications are a mixture close to pure iodine in the bottom product and a ternary hydroiodic acid -

hydrogen - water mixture in the distillate product. They belong to the region where the thermodynamic model is considered as reliable. Consequently, the next design steps are performed below so that the column mass balance lies in the reliable region. As we aim to get a residue exempt from the reactant HI, in order to increase the HI conversion, we then consider pure iodine at the bottom.

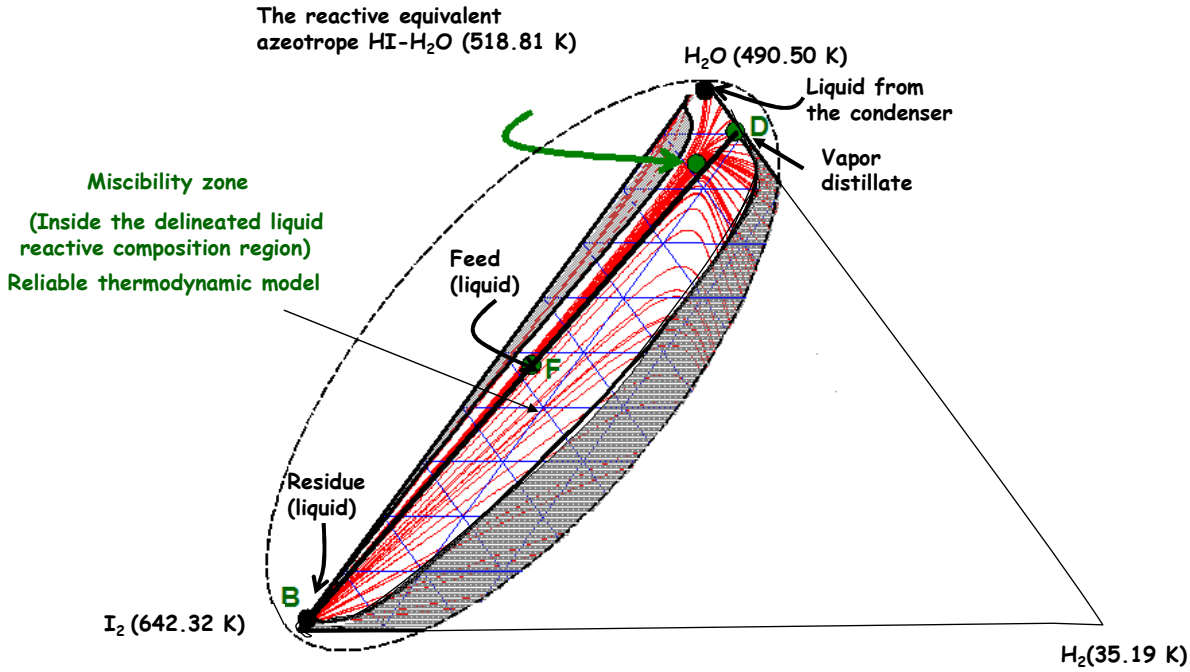

Figure 11. Neumann's thermodynamic model validity region of the quaternary HI-H_2-I_2-H_2O system under 22 bars

The set of attainable product compositions is presented in Table 2 and calculated so as to satisfy the several specifications, namely, HI dissociation yield of 99.6% molar; 100% I_2 recovery ratio in the bottom product and 99% molar I_2 purity in the bottom product.

Table 2: Production of hydrogen- P=22 bars-set of attainable products

- input data for the synthesis step

	Molar compositions		
	Liquid feed	Vapour distillate	Liquid residue
HI	0.10	$0.2\ 10^{-4}$	$0.85\ 10^{-3}$
H_2	0.00	$0.8962\ 10^{-1}$	0.00000
I_2	0.39	0.00000	0.99000
H_2O	0.51	0.91036	$0.915\ 10^{-2}$

4.3. Synthesis step

The set of attainable products obtained from the feasibility analysis step (Table 2) are exploited as starting data for the synthesis step based on the boundary value design (BVD) method. From these data, the composition and temperature profiles in the different sections of the column are computed stage by stage for different values of the variable parameter of the method : the reboil ratio noted s. The feed of the column is at its boiling temperature. A partial condenser is considered.

The first purpose of the boundary value design method consist in determining the minimum reboil ratio.

The vapour reactive stripping profile (full circles) and the vapour reactive rectifying profile (empty circles) are represented on figure 12 for reboil ratio values above and below its minimum value. The preset residue liquid composition is also displayed on figure 12.

At the minimum reboil ratio of about 5.573 an infinite number of stages is required to perform the separation. Above this value, the profiles intersect and the process is feasible. Hereafter, an effective reboil ratio of s=8 is considered.

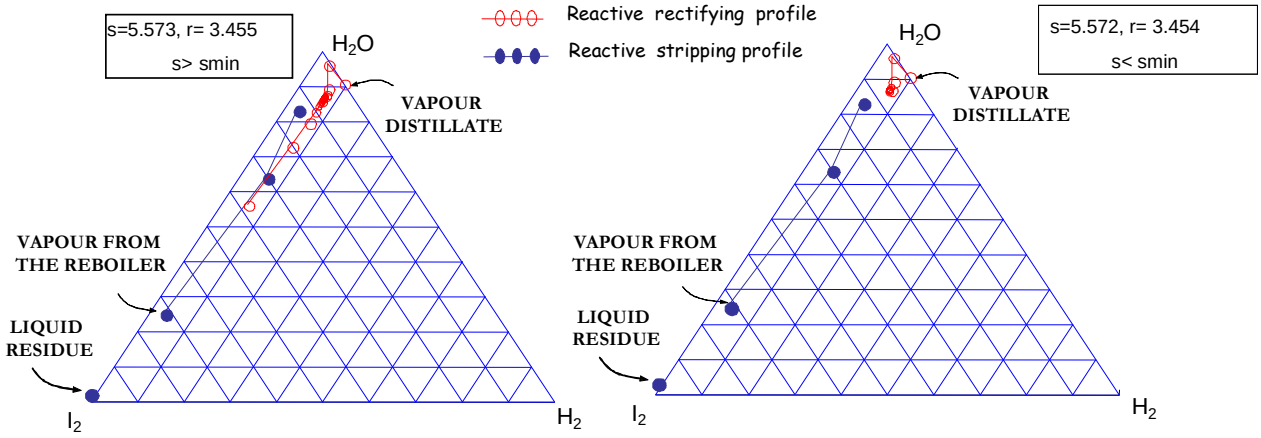

Figure 12. Vapour reactive profile in the reactive distillation column of a ternary HI-I_2-H_2O mixture for $s<s_{min}$ and $s>s_{min}$

The corresponding calculated reflux ratio is r=5.39 and the reactive rectifying and reactive stripping profiles are represented in the diagram on figure 13. The resulting configuration consists of 9 reactive rectifying stages (including the condenser) and 2 reactive stripping stages (including the boiler), with a feed at stage 10 (counted downwards).

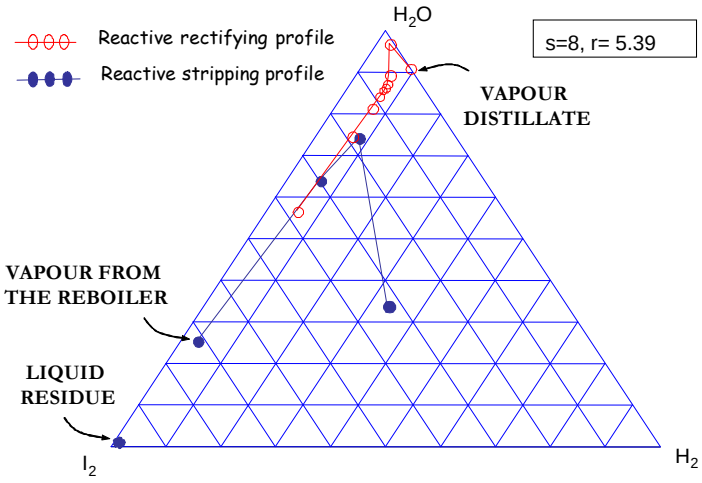

Figure 13. Vapour reactive profiles in the reactive distillation column of a ternary HI-I_2-H_2O mixture for s=8 and r=5.39

The resulting vapour composition profiles are presented on figure 14. Despite the high HI dissociation yield specified (99.6% molar), the hydrogen content remains low because of the low HI content in the

feed (10% molar). Besides, because of the high volatility of water versus iodine, the water content in the vapour phase showed in figure 14 remains very high.

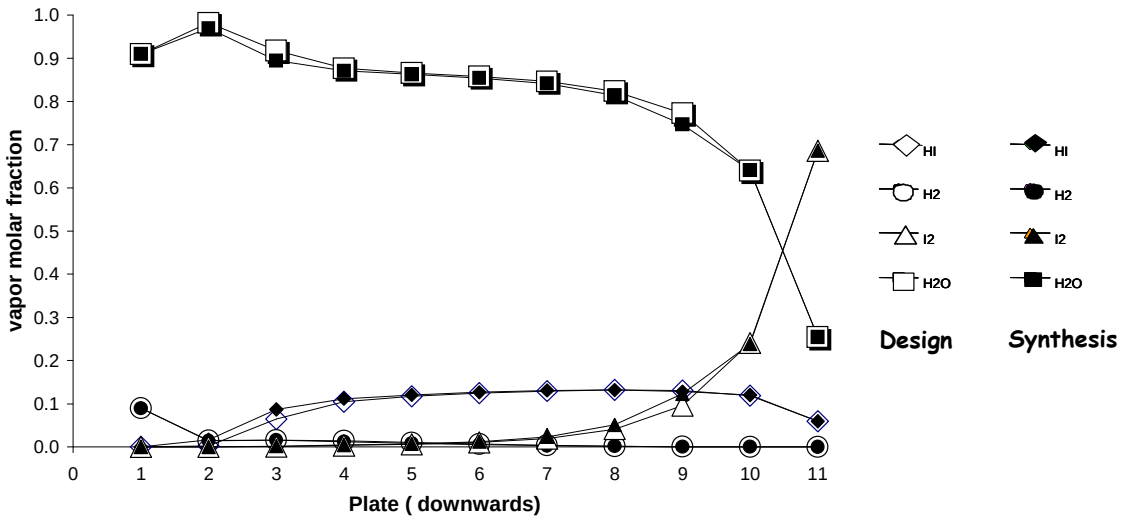

Figure 14. Comparison of the reactive profiles from the synthesis and design steps in the reactive distillation column of a ternary HI-I_2-H_2O mixture

A zoom on the composition displayed in figure 14 is shown in figure 15 to be able to analyze the HI, I_2 and H_2 vapour composition profile in the column. This figure shows that hydrogen production is obtained only for very low iodine content in the rectifying section because, in this condition, the reaction equilibrium is shifted towards the production of hydrogen, according to Le Chatelier's law. HI decomposition mostly occurs in the upper rectifying part of the column that lead to the recovery of hydrogen. In the stripping section, almost pure iodine is recovered at the bottom in the liquid residue.

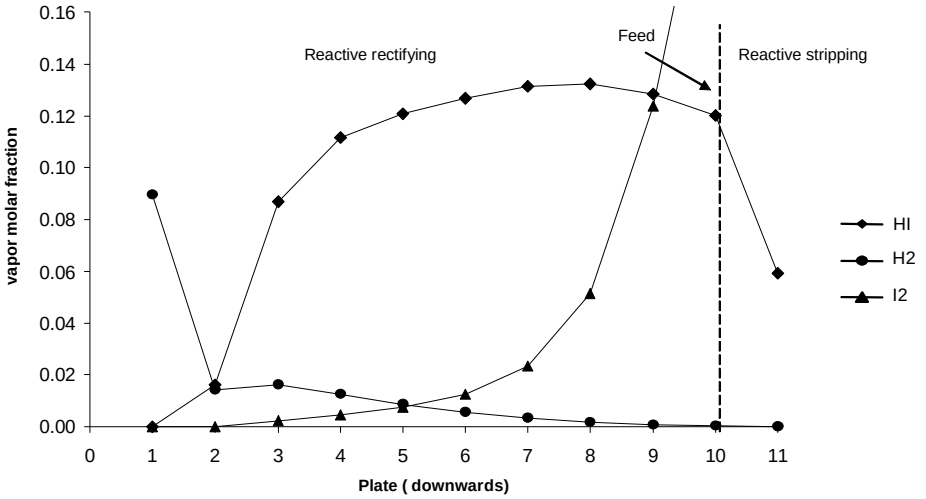

Figure 15. Zoom on the vapour composition profile in the reactive distillation column of a ternary HI-I_2-H_2O mixture

4.4. Design step

The previous step leads to a column configuration and a reboil ratio that permits to reach the initial specifications. But these results have been obtained neglecting all thermal phenomena (heat of reaction, difference between components vaporisation enthalpy). Based on ProSimPlus simulations [25], the design step recalculates the operating parameters without modifying the column configuration but taking into account heat balances.

In order to saturate the two degrees of freedom, the partial molar flow rate of H_2 in the distillate is set equal to 4.98 mol/s (for a molar feed flow of 100 mol/s) corresponding to the HI molar dissociation yield of 99.6% and a molar purity of I_2 in the bottom equal to 99% molar.

The resulting reflux ratio considering a heat effect is equal to 5.00 and is close to the reflux ratio obtained through the synthesis step of 5.39. That means that the assumptions formulated in the synthesis step are validated. Indeed, the thermal effects of the studied system are not so important (low endothermic heat of reaction and low difference between components vaporisation enthalpy).

Figure 14 compares the vapour profiles obtained through the synthesis and the design step. Both profiles are very similar. The temperature profile along the column is showed on figure 16. The temperature

increase observed in the lower part of the column can be related to the increase in the heavy boiling compound iodine content. In the upper part of the column, the temperature decrease is related to the increase in the light boiling compound hydrogen content.

Figure 17 presents the vapour and liquid composition profile in the column in the reactive composition space. It shows that both liquid and vapour profile belong to the vapour-liquid region with a turning in the vicinity of the equivalent reactive azeotrope behaving as an attraction point as mentioned above.

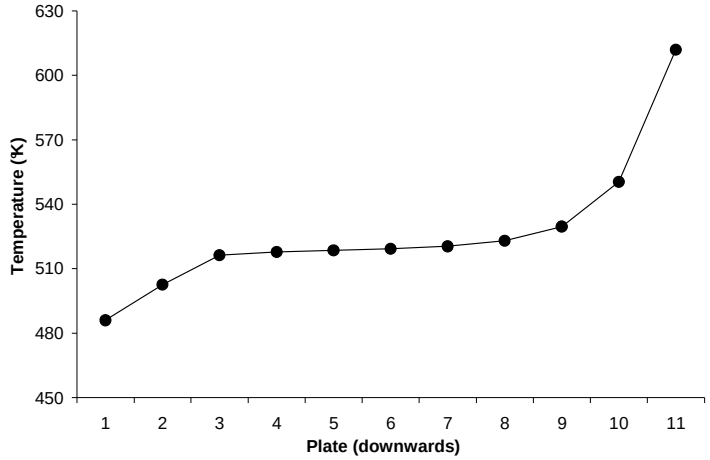

Figure 16. Temperature profile in the reactive distillation column of a ternary HI-I_2-H_2O mixture

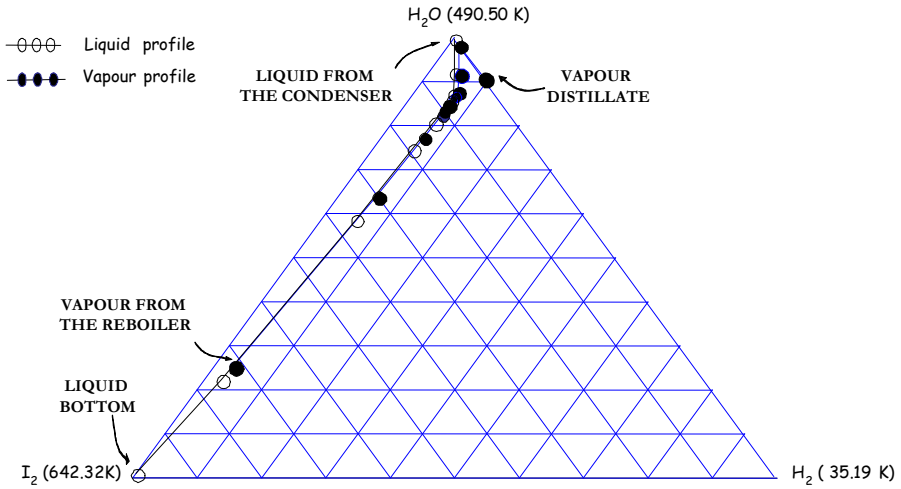

Figure 17. Vapour and liquid composition profile in the reactive composition space for the reactive distillation of a ternary HI-I_2-H_2O mixture

Table 3 summarises the configuration, operating parameters and performances of the process while figure 18 presents a detailed column configuration with operating parameters, molar compositions, temperatures and molar flows of the feed (F), distillate (D) and the residue (B).

Table 3: Operating parameters and performance of the column for a feed flow rate of 100 mol/s

Operating parameters of the column		Amount of H_2 produced (mol/s)	Molar HI dissociation yield in %
Reflux ratio	Number of stages		
5.00	11	4.98	99.6

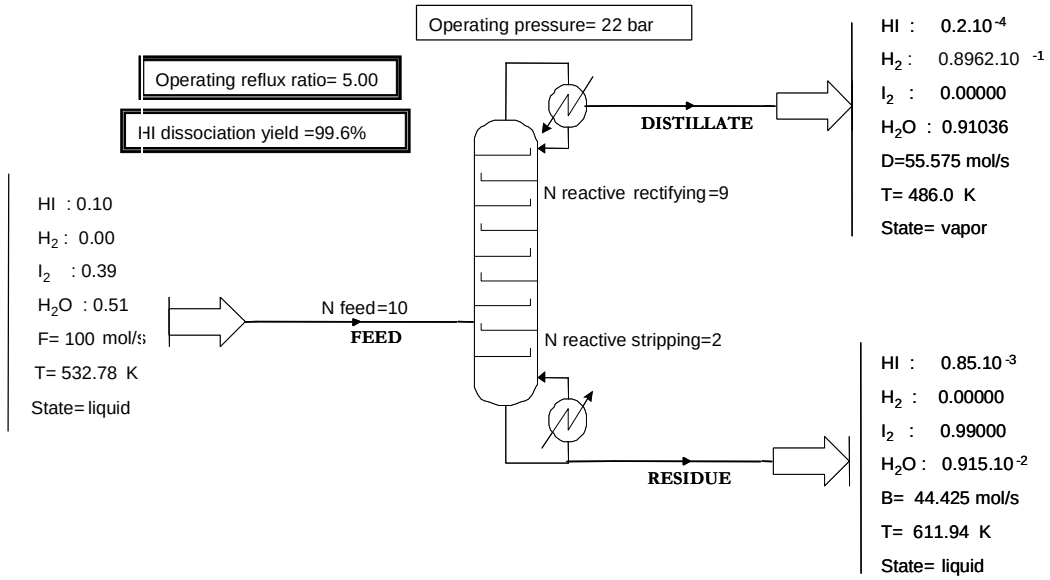

Figure 18. Detailed design results for the reactive distillation of a ternary HI-I_2-H_2O mixture – configuration and operating parameters

CONCLUSIONS AND OUTLOOKS

An extended global design approach for the feasibility, synthesis and design of reactive distillation columns involving vapour phase chemical reactions is applied to the vapour phase decomposition of HI to produce H_2. From minimal information concerning the physicochemical properties of the system, three successive steps lead to the design of the unit and the specification of its operating conditions: the feasibility analysis based on the analysis of reactive condensation curve map method (rCCM), the synthesis step based on the boundary value design method (BVD) and the design step based on rigorous simulations. Thanks to the application of the design approach, better performances in term of HI conversion rate are found than those of the initial reactive distillation column proposed by Roth and Knoche [24].

A feasible reactive distillation column configuration is proposed, for a residue consisting in pure iodine, under a pressure of 22 bars and for a fixed feed composition coming from the Bunsen reaction. This configuration can not be considered as an optimal design and can be used as a good initialization point for an MINLP optimization procedure. The influence of the pressure and the feed composition on the configuration and operating parameters of the reactive distillation column are planned to be studied.

It would be interesting to integrate the column configuration with side stream in the design methodology, in order to explore the possible improvement of the column configuration where H_2O is recovered in the side stream, H_2 at the top of the column and I_2 at the bottom.

Performance increase with potential modification of the original process of the HI concentration and decomposition section is expected.

REFERENCES

[1] Norman, J.H., G.E.Besenbruch and D.R. O'Keefe, Thermochemical water- Splitting Cycle for hydrogen production, GRI-A 16713 (1981)

[2] D. O'Keefe, C. Allen, G. Besenbruch, L. Brown, J. Norman, R. Sharp and K. McCorckle, Preliminary results from bench scale testing of a sulfur iodine thermochemical water splitting cycle, Int. J. of Hydrogen Energy, 7 (1982) 381-392.

[3] G. Arifal, J. Hwang and K. Onuki, Electro-electrodialysis of hydroiodique acid using the cation exchange membrane cross-linked by accelerated electron radiation. Journal of membrane science, 201 (2002) 39-44.

[4] K. Onuki, G. Hwang, G. Arifal and S. Shimizu, Electro-electrodialysis of hydroiodic acid in the presence of iodine at elevated temperature, Journal of membrane science, 192 (2001) 193-199.

[5] G. Hwang and K. Onuki, Simulation study on the catalytic decomposition of hydrogen iodide in the membrane reactor with a silica membrane for the thermochemical water-splitting IS process, Journal of membrane science, 194 (2001) 207-215.

[6] M. Roth and K.F. Knoche, Thermochemical water splitting through direct HI decomposition from H_2O-HI-I_2 solutions, Int. J. Hydrogen Energy, 14(8) (1989) 545-549.

[7] R. Thery, X.M. Meyer, X. Joulia and M. Meyer, Preliminary Design of reactive distillation columns, Chem. Eng. Res. Des., 83(A4) (2005) 379-400.

[8] F.C. Kracek, Solubilities in the system water-iodine to 200°C, J. Phys. Chem., 35 (1931) 417

[9] G. Wuster, Dissertation, RWTH- Aachen, 1979.

[10] C. Vanderzee, L. Gier, The enthalpy of solution of gaseous hydrogen iodide in water, and the relative apparent molar enthalpies of hydroiodic acid, J. Chem. Thermodyn., 6 (1974) 441-452

[11] H. Engels and K. F. Knoche, Vapour pressures of the system H_2O-HI-I_2 system and H_2, Int. J. of Hydrogen Energy, 11 (1986) 703-707.

[12] P.M Mathias, Applied thermodynamics in chemical technology: current practice and future challenges, Fluid Phase Equilibria, 228-229 (2005) 49-57.

[13] C. Berndahauser and K.F. Knoche, Experimental investigations of thermal HI decomposition from H_2O- HI-I_2 solutions, Int. J. Hydrogen Energy, 19(3) (1989) 239-244

[14] D. O'Keefe, J. H. Norman, D. G. Williamson., Catalysis research in thermochemical water-splitting processes, Catal. Rev. Sci. Eng., 22(3) (1980) 325-369.

[15] Neumann, Diplomaufgabe, RWTH Aachen, 28-01-1987.

[16] C.P.Almeida-Rivera., P.L.J. Swinkels., Grievink J., Designing reactive distillation processes: present and future, Comp. Chem. Eng., 28 (2004) 1997-2020.

[17] R. Thery, X.M. Meyer and X. Joulia, Analyse de faisabilité, Synthèse et Conception de procédés de distillation réactive: état de l'art et analyse critique, Can. Jour. Chem. Eng., 83 (2005) 242-266.

[18] B.Belaissaoui, Extension of a reactive distillation process design methodology: application to the hydrogen production through the iodine-sulfure thermochemical cycle, thèse de l'Institut National Polytechnique de Toulouse, 2006INPT003G, 2006.

[19] D. Barbosa and M.F. Doherty, The simple distillation of homogeneous reactive mixtures, Chem. Eng. Sci., 43(3) (1987a) 541-550.

[20] V.N. Kiva, E.K. Hilmen and S. Skogestad, Azeotropic phase equilibrium diagrams: a survey. Chem. Eng. Sci., 58 (2003) 1903-1953.

[21] Yu.A.Pisarenko, L.A.Serafimov, C.A.Cardona, D.L.Efremov and A.S.Shuwalov, Reactive distillation design: analysis of the process statics Reviews in chemical enginnering, 17(4) (2001) 253-327.

[22] D. Barbosa, M.F. Doherty, Design and minimum reflux calculations for single-feed multicomponent reactive distillation columns, Chem. Eng. Sci., 43(7) (1987b) 1523-1537.

[23] D. Barbosa, M.F. Doherty, Design and minimum reflux calculations for double-feed multicomponent reactive distillation columns, Chem. Eng. Sci., 43(9) (1987c) 2377-2389.

[24] D. Barbosa and M.F. Doherty, A new set of composition variables for the representation of reactive phase diagrams, Proc. R. Soc. Lond., A413 (1987d) 459-464.

[25] http://www.prosim.net

[26] Ung S.,Doherty M.F., Synthesis of reactive distillation systems with multiple equilibrium chemical reactions, Ind. Eng.Chem. Res, 34, (1995) 2555-2565

FIGURES CAPTION

Figure 1. The principle of the thermochemical water decomposition cycle for hydrogen production

Figure 2. Concept of the Sulfur / Iodine thermochemical cycle for the production of hydrogen

Figure 3: Integration of a reactive distillation in the Sulfur / Iodine thermochemical cycle for the production of hydrogen

Figure 4. Description of the complex phase behaviour of the HI-H_2-I_2-H_2O system

Figure 5. Diagram P-x-y of HI-H_2O. Comparison of the Neumann's thermodynamic model calculation to experimental data of Engels and Knoche (1986)

Figure 6. Methodology for the design of vapour phase reactive distillation processes.

Figure 7. Non reactive condensation curve map of the ternary HI-I_2-H_2O system under 22 bars

Figure 9. Reactive condensation curve map (rCCM) of the HI-H_2-I_2-H_2O system under 22 bars.

Figure 10. X_{I_2} - Y_{I_2} diagram of the HI-H_2-I_2-H_2O system under 22 bars

Figure 11. Neumann's thermodynamic model validity region of the quaternary HI-H_2-I_2-H_2O system under 22 bars

Figure 12. Vapour reactive profile in the reactive distillation column of a ternary HI-I_2-H_2O mixture for $s<s_{min}$ and $s>s_{min}$

Figure 13. Vapour reactive profiles in the reactive distillation column of a ternary HI-I_2-H_2O mixture for s=8 and r=5.39

Figure 14. Comparison of the reactive profiles from the synthesis and design steps in the reactive distillation column of a ternary HI-I_2-H_2O mixture

Figure 15. Zoom on the vapour composition profile in the reactive distillation column of a ternary HI-I_2-H_2O mixture

Figure 16. Temperature profile in the reactive distillation column of a ternary HI-I_2-H_2O mixture

Figure 17. Vapour and liquid composition profile in the reactive composition space for the reactive distillation of a ternary HI-I_2-H_2O mixture

Figure 18. Detailed design results for the reactive distillation of a ternary HI-I_2-H_2O mixture – configuration and operating parameters

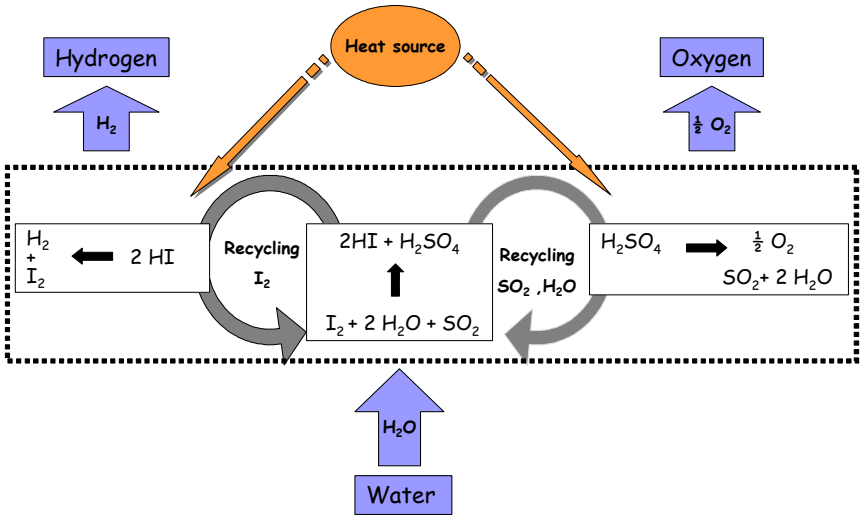

Figure 1. The principle of the thermochemical water decomposition cycle for hydrogen production

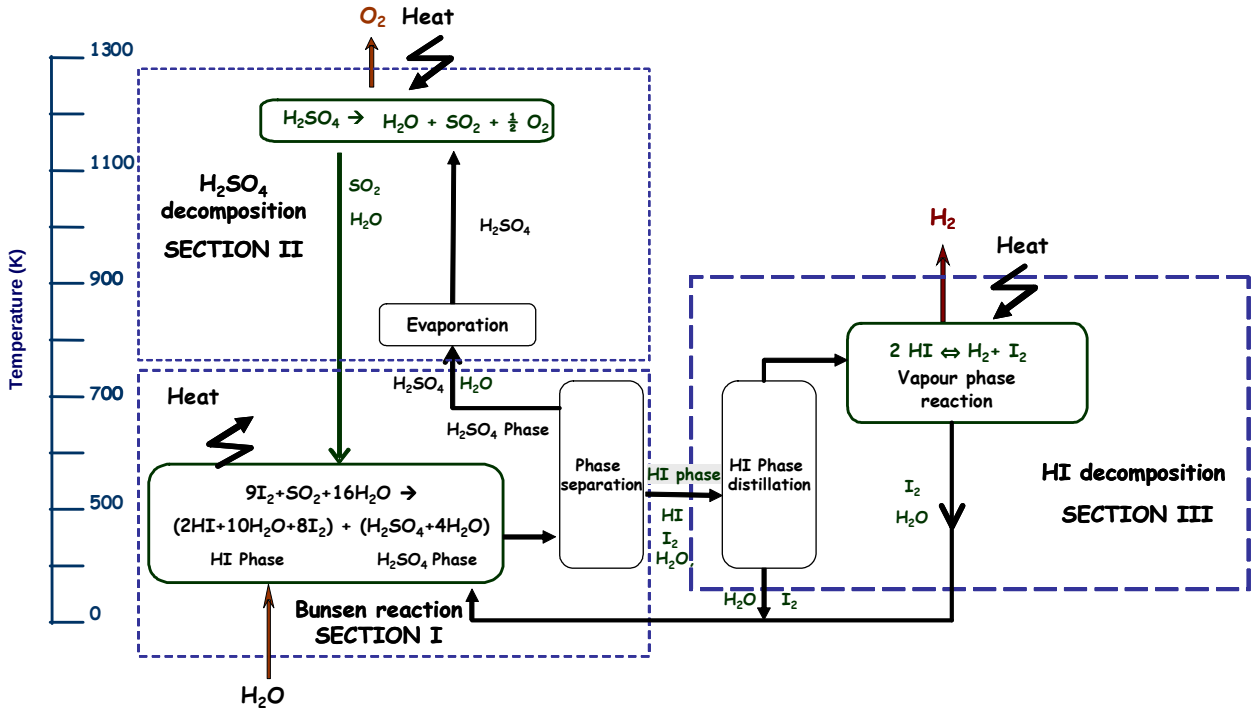

Figure 2. Concept of the Sulfur / Iodine thermochemical cycle for the production of hydrogen

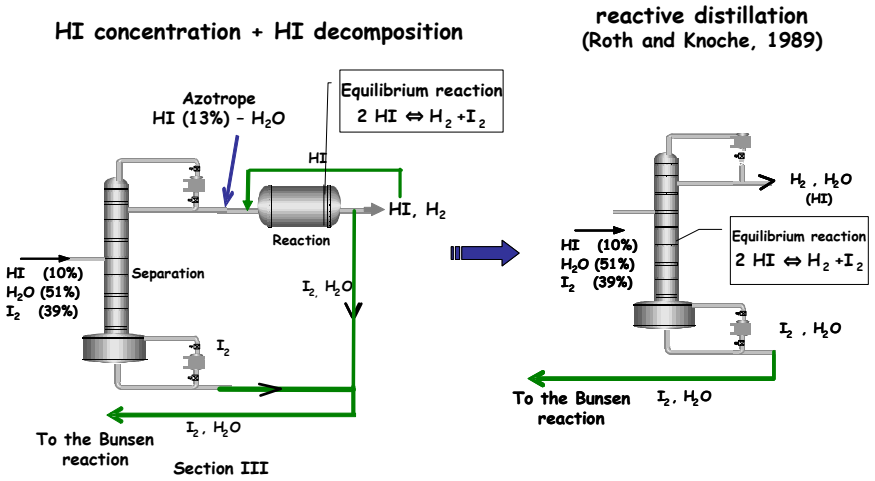

Figure 3: Integration of a reactive distillation in the Sulfur / Iodine thermochemical cycle for the production of hydrogen

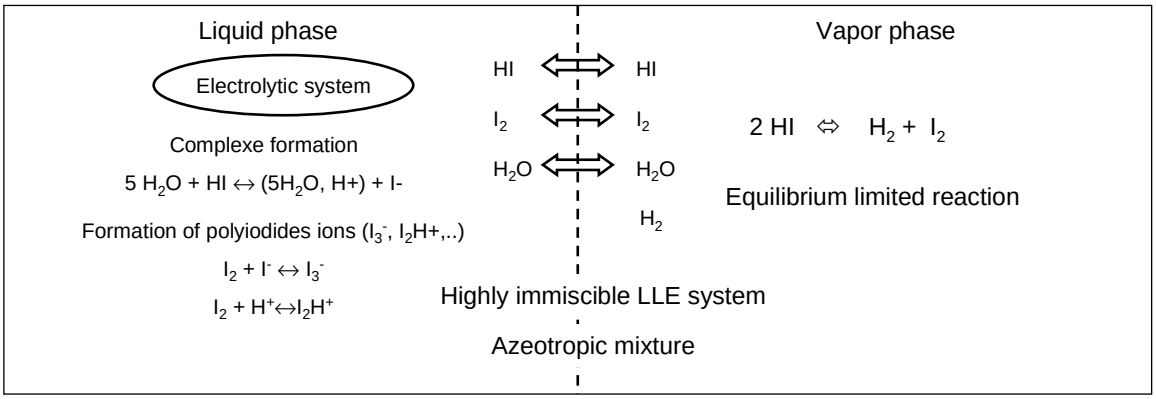

Figure 4. Description of the complex phase behaviour of the HI-H_2-I_2-H_2O system

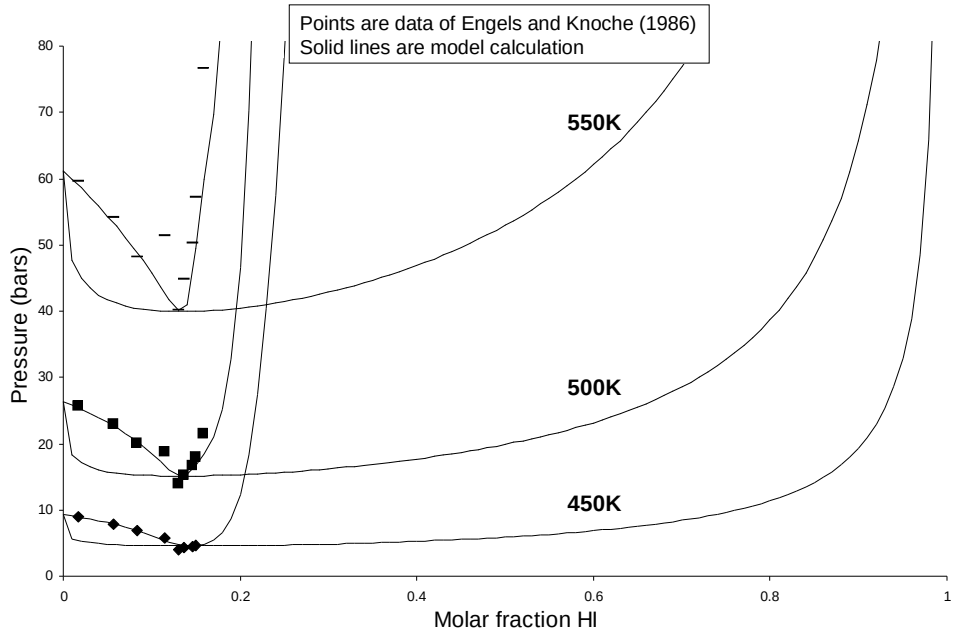

Figure 5. Diagram P-x-y of HI-H_2O. Comparison of the Neumann's thermodynamic model calculation to experimental data of Engels and Knoche (1986)

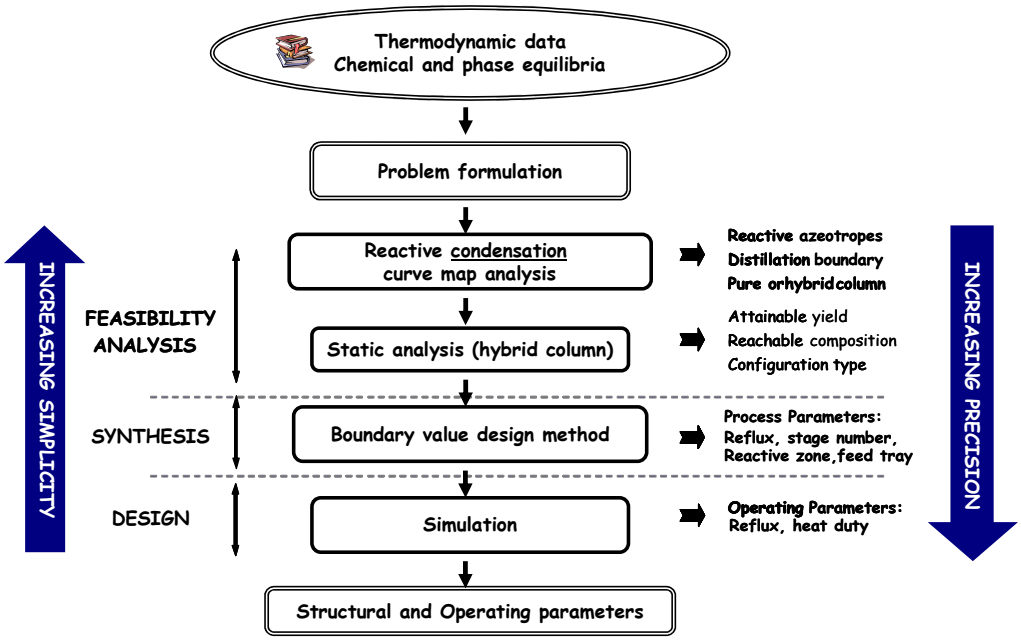

Figure 6. Methodology for the design of vapour phase reactive distillation processes.

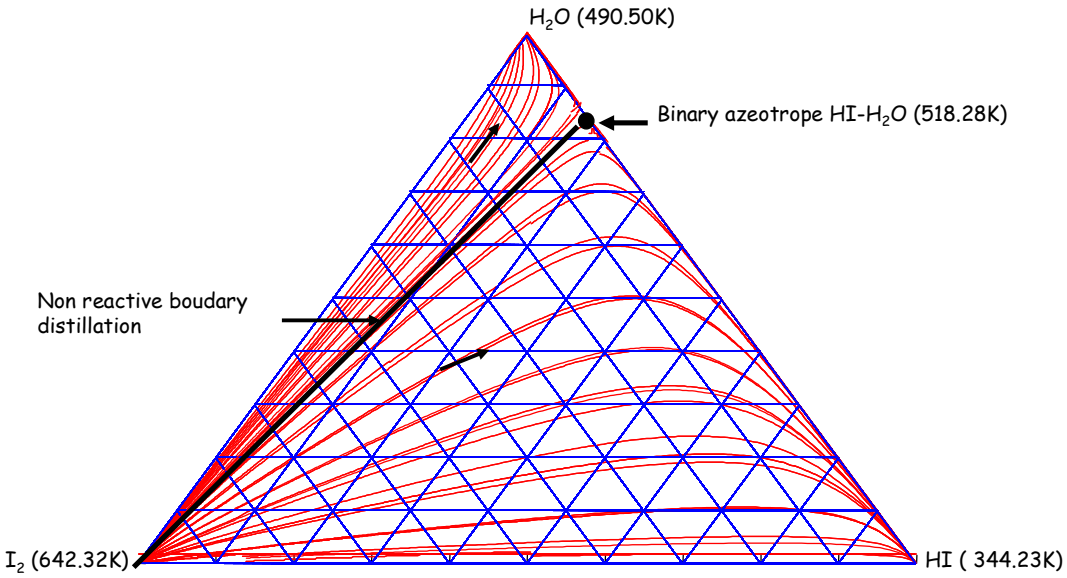

Figure 7. Non reactive condensation curve map of the ternary HI-I_2-H_2O system under 22 bars

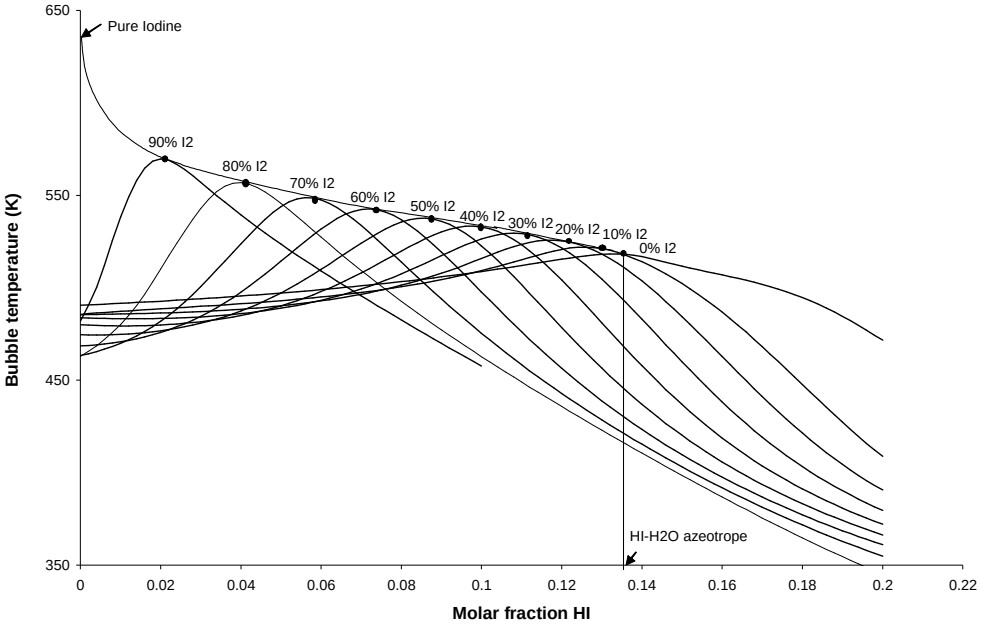

Figure 8. Influence of I_2 concentration on the maximum bubble temperature of the non reactive ternary system HI-I_2-H_2O

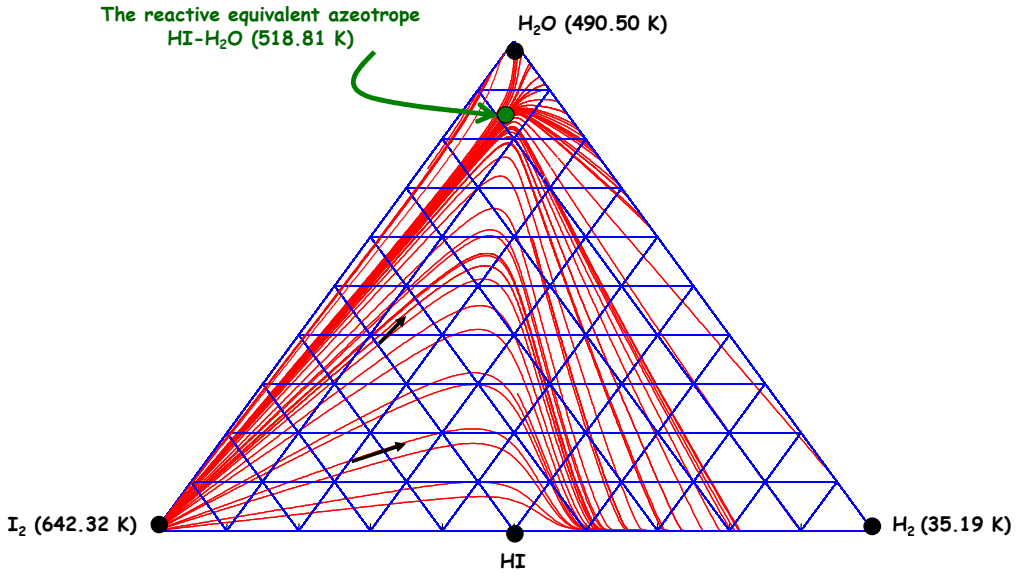

Figure 9. Reactive condensation curve map (rCCM) of the HI-H_2-I_2-H_2O system under 22 bars.

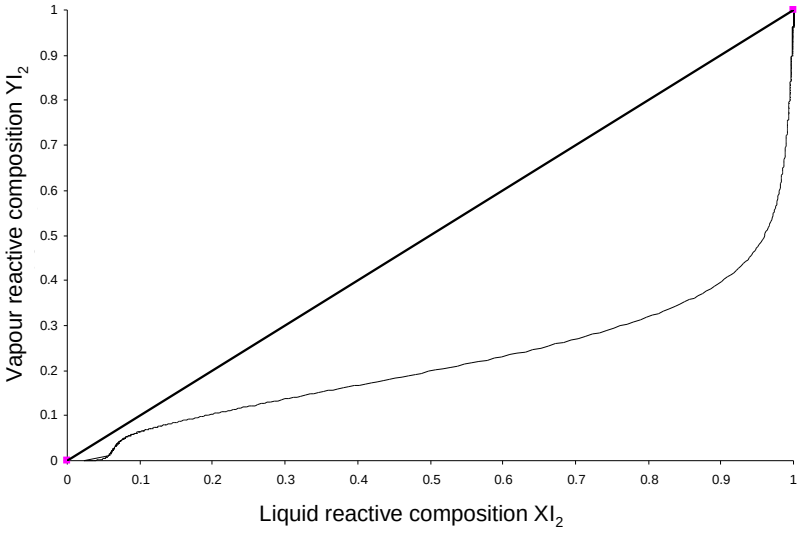

Figure 10. X_{I_2} - Y_{I_2} diagram of the HI-H_2-I_2-H_2O system under 22 bars

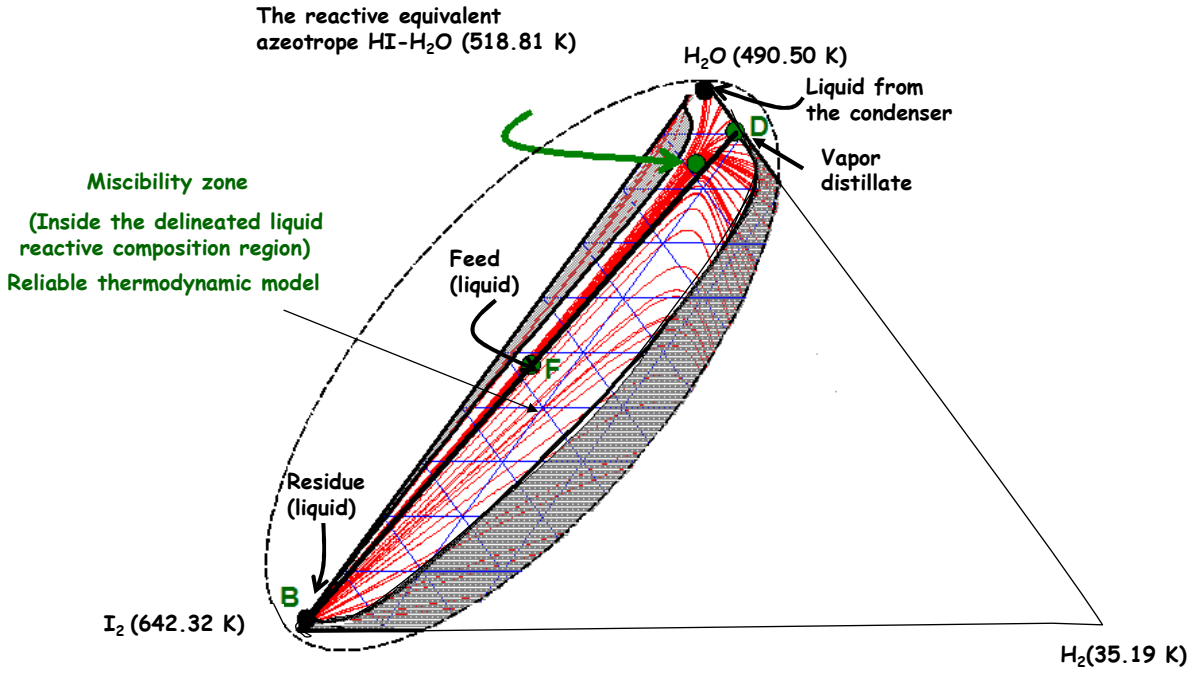

Figure 11. Neumann's thermodynamic model validity region of the quaternary HI-H_2-I_2-H_2O system under 22 bars

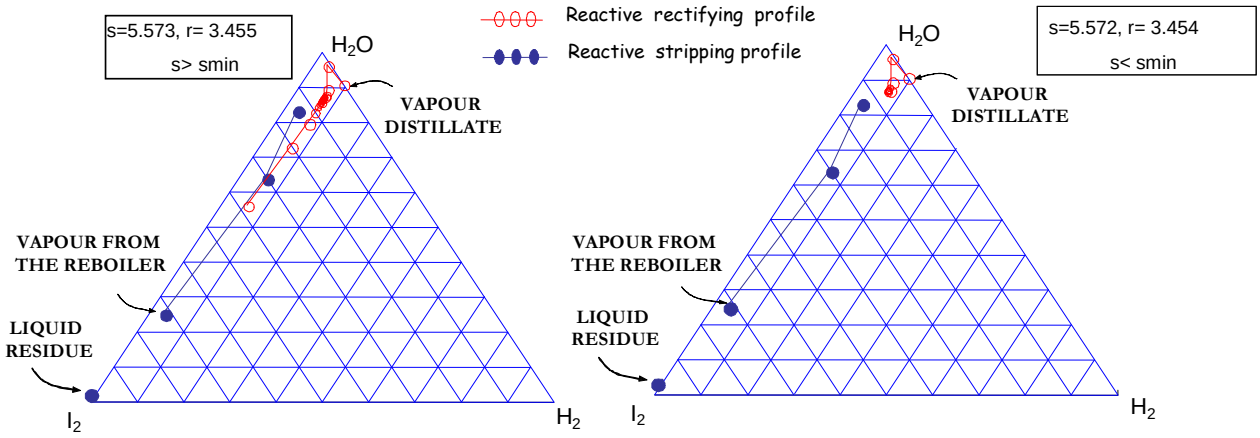

Figure 12. Vapour reactive profile in the reactive distillation column of a ternary HI-I_2-H_2O mixture for $s<s_{min}$ and $s>s_{min}$

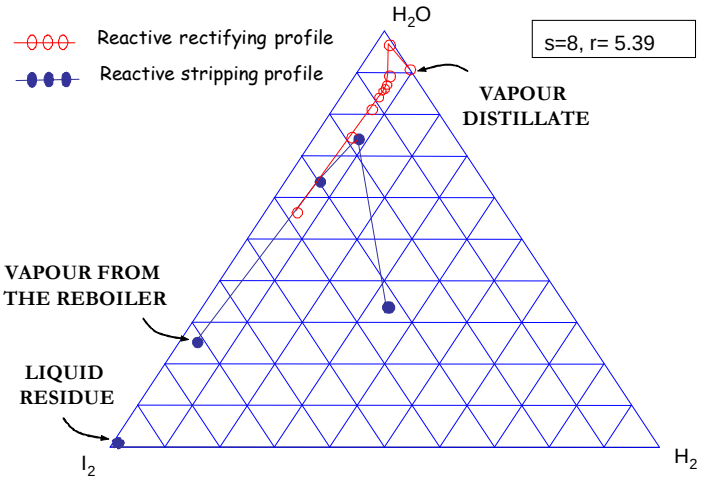

Figure 13. Vapour reactive profiles in the reactive distillation column of a ternary HI-I_2-H_2O mixture for s=8 and r=5.39

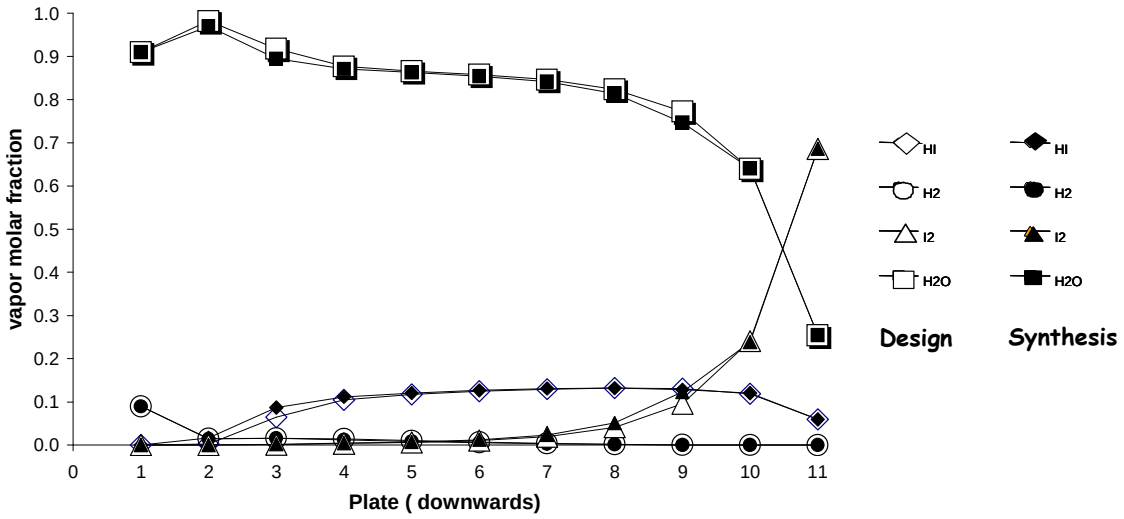

Figure 14. Comparison of the reactive profiles from the synthesis and design steps in the reactive distillation column of a ternary HI-I_2-H_2O mixture

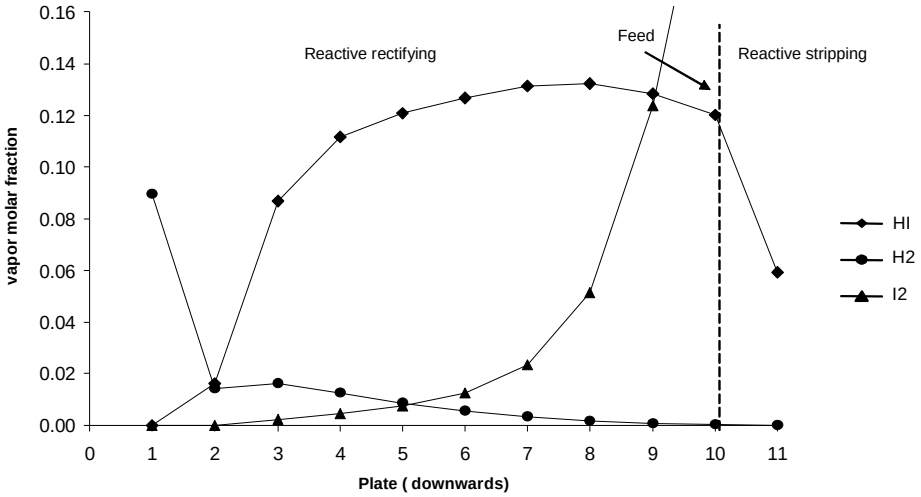

Figure 15. Zoom on the vapour composition profile in the reactive distillation column of a ternary HI-I_2-H_2O mixture

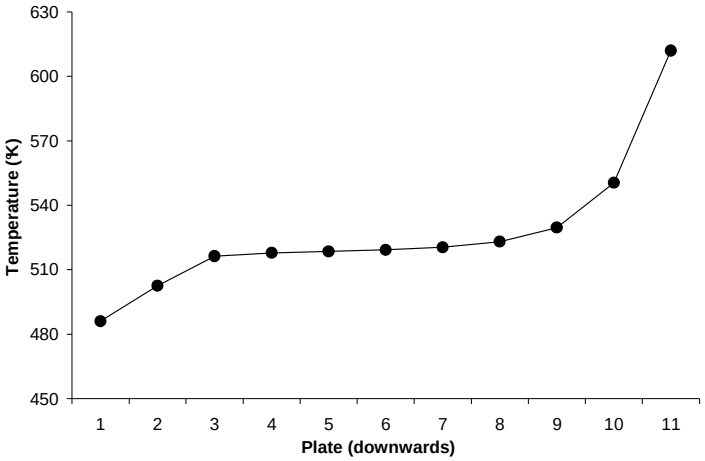

Figure 16. Temperature profile in the reactive distillation column of a ternary HI-I_2-H_2O mixture

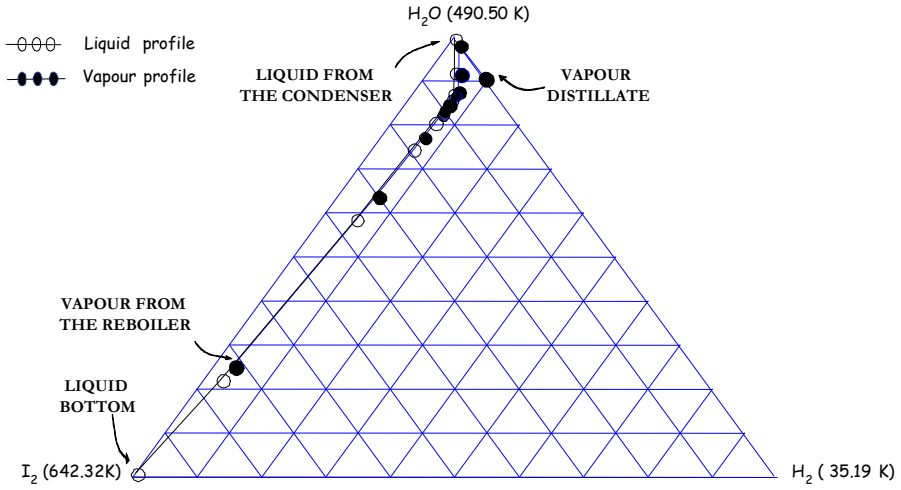

Figure 17. Vapour and liquid composition profile in the reactive composition space for the reactive distillation of a ternary HI-I_2-H_2O mixture

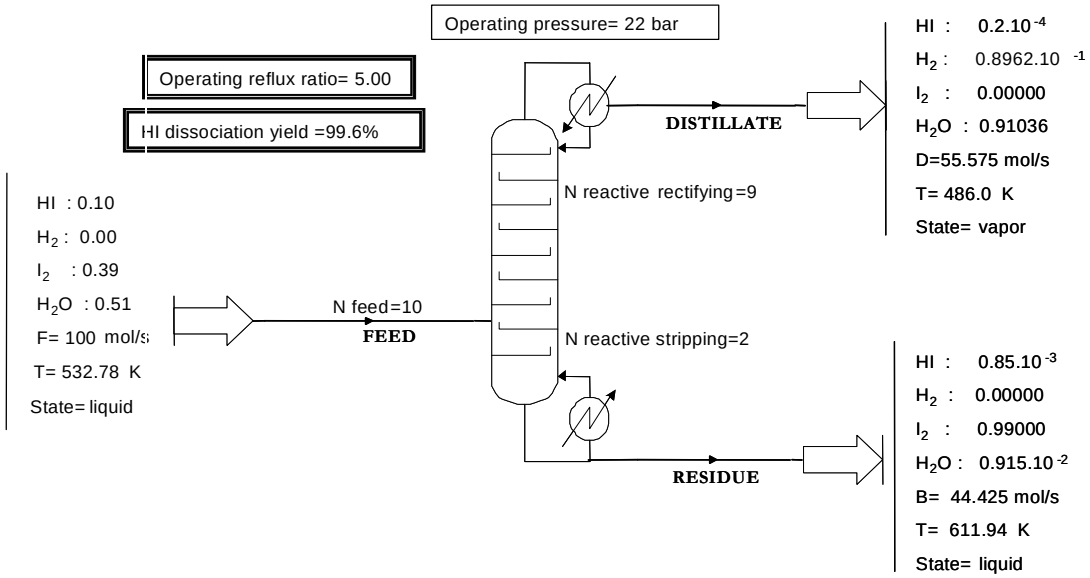

Figure 18. Detailed design results for the reactive distillation of a ternary HI-I_2-H_2O mixture – configuration and operating parameters

TABLES CAPTION

Table 1. Vapor physical composition of the reactive pseudo-azeotrope compared to the binary azeotrope (P=22bars)

Table 2: Production of hydrogen- P=22 bars-set of attainable products-input data for the synthesis step

Table 3: Operating parameters and performance of the column for a feed flow rate of 100 mol/s

Table 1. Approximated vapor physical composition of the equivalent reactive azeotrope compared to the binary azeotrope (P=22bars)

	HI	H_2	I_2	H_2O
Equivalent reactive azeotrope	0.1170	0.0080	0.0080	0.8670
Binary azeotrope	0.1330	0.0000	0.0000	0.8670

Table 2: Production of hydrogen- P=22 bars-set of attainable products

- input data for the synthesis step

	Molar compositions		
	Liquid feed	Vapour distillate	Liquid residue
HI	0.10	$0.2\ 10^{-4}$	$0.85\ 10^{-3}$
H_2	0.00	$0.8962\ 10^{-1}$	0.00000
I_2	0.39	0.00000	0.99000
H_2O	0.51	0.91036	$0.915\ 10^{-2}$

Table 3: Operating parameters and performance of the column for a feed flow rate of 100 mol/s

Operating parameters of the column		Amount of H_2 produced (mol/s)	Molar HI dissociation yield in %
Reflux ratio	Number of stages		
5.00	11	4.98	99.6